NIH Public Access
Author Manuscript
Nanomedicine (Lond). Author manuscript; available in PMC 2012 August 01.

Published in final edited form as:
Nanomedicine (Lond). 2012 July ; 7(7): 1017–1028. doi:10.2217/nnm.11.179.

Multifunctional nanoagent for thrombus-targeted fibrinolytic therapy

Jason R. McCarthy[1,*], **Irina Y. Sazonova**[3], **S. Sibel Erdem**[1], **Tetsuya Hara**[2], **Brian D. Thompson**[1,4], **Purvish Patel**[2], **Ion Botnaru**[2], **Charles P. Lin**[1,4], **Guy L. Reed**[5], **Ralph Weissleder**[1], and **Farouc A. Jaffer**[2,4,*]

[1]Center for Systems Biology, Harvard Medical School and Massachusetts General Hospital, 149 13th St., 6th Floor, Charlestown, MA 02129, USA

[2]Cardiovascular Research Center, Cardiology Division, Harvard Medical School and Massachusetts General Hospital, Boston, MA

[3]Section of Cardiology, Department of Medicine, Medical College of Georgia, Georgia Health Sciences University, Augusta, GA

[4]Wellman Center for Photomedicine, Department of Dermatology, Harvard Medical School and Massachusetts General Hospital, Boston, MA

[5]Department of Medicine, The University of Tennessee Health Science Center, Memphis, TN

Abstract

Aims—Current thrombolytic therapies rely upon exogenous plasminogen activators (PA) to effectively lyse clots, thereby restoring blood flow and preventing tissue and organ death. Yet, these PAs may also impair normal hemostasis which may lead to life-threatening bleeding, including intracerebral hemorrhage. Thus, the aim of this current study is to develop new thrombus-targeted fibrinolytic agents that harness the multifunctional theranostic capabilities of nanomaterials, potentially allowing for the generation of efficacious thrombolytics while minimizing deleterious side effects.

Materials and Methods—A thrombus-targeted nano-fibrinolytic agent (**CLIO-FXIII-PEG-tPA**) was synthesized using a magnetofluorescent crosslinked dextran-coated iron oxide (CLIO) nanoparticle platform that was conjugated to recombinant tissue plasminogen activator (tPA). Thrombus-targeting was achieved by derivatizing the nanoparticle with an activated factor XIII (FXIIIa)-sensitive peptide based on the amino terminus of α_2-antiplasmin. Human plasma clot binding ability of the targeted and control agents was assessed by fluorescence reflectance imaging. Next, the in vitro enzymatic activity of the agents was assessed by S2288-based amidolytic activity, and an ELISA D-dimer assay for fibrinolysis. In vivo targeting of the nanoagent was next examined by intravital fluorescence microscopy of murine arterial and venous thrombosis. The fibrinolytic activity of the targeted nanoagent compared to free tPA was then evaluated in vivo in murine pulmonary embolism.

Results—In vitro, the targeted thrombolytic nanoagent demonstrated binding to fresh frozen plasma (FFP) clots superior to control nanoagents (ANOVA $p < 0.05$). On a weight (mg) basis, the

Tel.: 617-726-9218, Fax.: 617-643-6133, jason_mccarthy@hms.harvard.edu or fjaffer@mgh.harvard.edu.

Financial & competing interests disclosure

The authors have no relevant affiliations or financial involvement with any organization or entity with a financial interest in or financial conflict with the subject matter or materials discussed in the manuscript. This includes employment, consultancies, honoraria, stock ownership or options, expert testimony, grants or patents received or pending, or royalties. No writing assistance was utilized in the production of this manuscript.

NIH-PA Author Manuscript
NIH-PA Author Manuscript
NIH-PA Author Manuscript

NIH-PA Author Manuscript

NIH-PA Author Manuscript

NIH-PA Author Manuscript

S2288 amidolytic efficiency of the targeted nanoagent was approximately 15% reduced compared to free tPA. When normalized by S2288-based activity, targeted, control, and free tPA samples demonstrated equivalent in vitro fibrinolytic activity against human plasma clots, as determined by ELISA D-dimer assays. The FXIIIa targeted fibrinolytic nanoagent efficiently bound the margin of intravascular thrombi as detected by IVFM. In *in vivo* fibrinolysis studies normalized for activity, the FXIIIa-targeted agent lysed pulmonary emboli with similar efficacy as free tPA ($p>0.05$).

Conclusions—The applicability of a FXIIIa-targeted thrombolytic nanoagent in the treatment of thromboembolism was demonstrated in vitro and in vivo. Future studies are planned to investigate the safety profile and overall efficacy of this class of nanoagents, and to further optimize their thrombus-targeting profile and lytic action.

Keywords

Fibrinolytic; iron oxide; therapy; thrombosis; multimodal; theranostic; imaging

Introduction

Thrombosis is the formation of a blood clot (thrombus) within a vessel, and is a process that is naturally regulated by hemostasis between coagulation and fibrinolysis. When the normally beneficial hemostatic system becomes overwhelmed, however, pathological thrombi form and occlude blood flow, leading to ischemic arterial syndromes, such as stroke and myocardial infarction, as well as venous syndromes, including deep vein thromboses and resultant pulmonary emboli. Plasminogen activators (PAs) are used to trigger the dissolution of these thrombi (termed thrombolysis or fibrinolysis) by catalyzing the conversion of plasminogen to the protease plasmin, which then digests fibrin and lyses the clot. PA therapy aims to restore blood flow rapidly, and to thus reduce the large associated mortality and disability caused by vascular thrombi.

While this therapeutic application of PAs offers a clinically useful therapy, it is fraught with challenges. In fact, 20 % percent of infarct-related coronary arteries fail to re-establish normal coronary flow following tissue plasminogen activator (tPA) therapy [1]. In addition, another 15 percent of reperfused arteries will re-occlude, leading to acute myocardial infarction. If re-occlusion occurs, the benefits are reduced, as sustained patency is associated with the best prognosis [1]. Administration of tPA may also impair the normal hemostatic system, leading to life-threatening bleeding consequences, including intracerebral hemorrhage (ICH) [2]. In a 1995 stroke trial, thrombolytic therapy with tPA increased the symptomatic intracerebral hemorrhage (ICH) rate by 10-fold, occurring in 6.4% of tPA-treated patients as compared to 0.6% of those given placebo [2]. In a more recent study regarding PA treatment of myocardial infarction, the rate of ICH was ~1%, with 55% of ICH patients dying, and 55% of ICH survivors possessing residual neurological deficit [3]. It is therefore vital to develop new thrombolytic agents with potentially increased efficacy and fibrin specificity, greater therapeutic windows, and vastly improved safety profiles.

Nanomaterials are promising as a scaffold for building targeted thrombolytics [4–7]. For the most part, it is difficult to develop nanoagents that transverse the blood brain barrier (BBB) in the absence of permeabilization [8]. This may be due, in part, to the lack of an endogenous pathway for the particles to translocate into the brain. Thus, covalent attachment of thrombolytics to a targeted nanoparticulate delivery vehicle may lead to the development of agents minimizing the most egregious of side effects, ICH. Nanomaterials may also extend the circulation time of PAs, allowing them to be administered as a bolus as opposed to an infusion, increasing the duration of effect [9].

NIH-PA Author Manuscript

NIH-PA Author Manuscript

NIH-PA Author Manuscript

We have previously reported the synthesis and utility of magnetofluorescent nanoagents for the targeted molecular magnetic resonance and optical imaging of thrombi [10]. These particles, based upon crosslinked dextran coated iron oxide (CLIO) nanoparticles, were targeted to two different components of thrombi, namely fibrin and activated factor XIII (FXIIIa), via peptide affinity ligands. The latter target, blood transglutaminase FXIIIa is a hallmark of acute thrombi [11]. FXIIIa crosslinks fibrin strands, thereby stabilizing the nascent thrombus. FXIIIa also crosslinks α_2-antiplasmin into the clot, effectively increasing fibrinolytic resistance. Thus, a FXIIIa-targeted nanoagent, based upon the N-terminus of α_2-antiplasmin [12–14], may allow for the determination of clots that are younger and therefore more amenable to fibrinolysis. This same nanoscaffold may also serve as an efficient delivery vehicle for targeted thrombolysis, by locally concentrating PAs in freshly formed thrombi.

Herein, we discuss the synthesis, and in vitro and in vivo applicability of peptide targeted thrombolytic nanomaterials. These particles, functionalized with imaging, targeting, and therapeutic ligands using a layer-by-layer methodology, were assayed in vitro for clot binding and enzymatic activity, and compared to additional synthesized control agents. The in vivo targeting and thrombolytic potential of the nanoagent was also examined in murine models of arterial and venous thrombosis, and pulmonary embolism.

Materials and methods

General

All solvents and reagents, unless noted below, were purchased from Acros or Sigma Aldrich and were reagent grade or better and used as received. The discrete PEG reagent, Mal-dPEG$_{24}$-NHS, was purchased from Quanta BioDesign. Crosslinked iron oxide nanoparticles (CLIO) was synthesized as described previously, and were obtained from the Center for Systems Biology Chemistry Core [15–17]. All peptides were synthesized by the Peptide Synthesis/Protein Sequencing Core at the Massachusetts General Hospital using conventional Fmoc synthesis strategies on Rink amide resin. The sequences were as follows: FXIII -GNQEQVSPLTLLKC; CXIII – GNAEQVSPLTLLKC (Circ 2004, Bioconj 2009). The peptides (0.1 mmol scale) were received on resin with the N-terminus t-butoxycarbonyl (Boc)-protected. HPLC was performed on a Varian ProStar HPLC. Gradients were run with buffer A (H_2O/0.1% trifluoroacetic acid (TFA)) and buffer B (acetonitrile/10% buffer A/ 0.1% TFA). For analytical HPLC a Varian C-18 reverse phase column was used with dimensions of 250 mm × 4.6 mm. For semi-preparative HPLC a Varian C-18 reverse phase column was used with dimensions of 250 mm × 21.2 mm. UV-vis spectra were recorded on Cary 50 spectrophotometer, and fluorescence emission spectra on a Cary Eclipse spectrofluorometer. Electrospray ionization (ESI) mass spectra were recorded on a Waters Micromass ZQ Mass Spectrometer in the solvents indicated. The bifunctional PEG was purchased from Quanta Biodesign Limited. The tPA utilized was Alteplase from Genentech. Fluorescence reflectance imaging was accomplished on a Siemens BonSAI system in the far red channel (660 nm excitation/735 nm emission). The amount of protein per particle was calculated using the Bio-Rad Protein Assay Kit II (#500-0002). The tPA inhibitor PPACK (PI117-0005) was purchased from Enzo Life Sciences. The Subcommittee on Research Animal Care at Massachusetts General Hospital and IACUC of the Medical College of Georgia approved all animal procedures.

CLIO-VT680

To a suspension of CLIO (20 mg, 9.98 mg Fe/mL) in phosphate buffered saline (pH 7.4) was added the NIR fluorophore VivoTag 680 (1 mg, ex/em 673/691 nm, Perkin Elmer, Woburn, MA) in 100 μL dimethylsulfoxide (DMSO). The reaction was allowed to proceed

NIH-PA Author Manuscript

NIH-PA Author Manuscript

NIH-PA Author Manuscript

for 3 h, at which time the product was purified by size exclusion chromotography (Sephadex G-25, Dulbecco's Phosphate buffered saline, PBS) to give 3 dyes per particle, as determined spectrophotometrically.

Peptide cleavage and purification

The peptide resin was swelled in N,N-dimethylformamide (DMF) for 15 min and filtered. The peptide was then cleaved from the resin and simultaneously deprotected by reaction with TFA/triisopropylsilane/water (95:2.5:2.5, 5 mL) for 3 h. The resin was filtered, and the peptide contained in the supernatant was precipitated by addition of excess methyl tert-butyl ether (MTBE). The precipitate was recovered following centrifugation and washing twice more with MTBE. The resulting crude peptide was purified by HPLC, as described previously [10].

Peptide-modified CLIO (CLIO-FXIII and CLIO-CXIII)

To a suspension of **CLIO-VT680** (10 mg, 9.4 mg Fe/mL) in PBS (pH 7.4) was added succinimidyl iodoacetate (SIA, 10 mg) in 400 μL DMSO. The reaction proceeded for 4 hours, and was then purified by size exclusion chromatography (Sephadex G-25, PBS). To the resulting suspension was added the respective peptide (10 mg). The reaction was allowed to proceed for 16 h, and was also purified by size exclusion chromatography (Sephadex G-25, PBS). The number of peptides per particle was determined spectroscopically, after modification with fluorescein isothiocyanate (FITC). To the peptide labeled particles (1 mg in 600 μL PBS) was added FITC (0.1 mg in 250 μL DMSO). The reaction was allowed to proceed for 16 h, at which point it was purified via filtration through Sephadex G25 to give the N-terminal dye-labeled species.

Addition of discrete PEG linker (CLIO-FXIII-PEG, CLIO-CXIII-PEG, and CLIO-PEG)

To a suspension of **CLIO-FXIII, CLIO-CXIII** or **CLIO-VT680** (9 mg, 7 mg Fe/mL) in PBS (pH 7.4) was added Mal-dPEG$_{24}$-NHS ester (0.9 mg) in 240 μL DMSO. The reaction was allowed to proceed for 3 h, at which time it is purified by size exclusion chromatography (Sephadex G-25, PBS). The number of peptides per PEG was determined spectroscopically, after modification with (N-Fluoreceinthioureido)-2-mercaptoethylamine [18]. To the PEG-modified particle (1 mg in 570 μL PBS) was added the thiol-modified fluorescein derivative (0.1 mg in 230 μL DMSO). The reaction was allowed to proceed for 16 h, at which point it was purified via filtration through Sephadex G25 to give the dye-labeled species.

Addition of tPA to PEG-modified nanoagents (CLIO-FXIII-PEG-tPA, CLIO-CXIII-PEG-tPA, and CLIO-PEG-tPA)

A suspension of **CLIO-FXIII-PEG, CLIO-CXIII-PEG,** or **CLIO-PEG** (9 mg, 15 mg Fe/mL) in PBS (pH 7.4) was added to a solution of tPA (6 mg, 1 mg/mL in sterile water). The resulting solution was exchanged into Tris buffer (pH 7.5) by centrifugal concentration (Waters, 4 kD cutoff) and dilution with Tris buffer (3 rounds of washing). The resulting solution was allowed to react for 24 h, and was purified by centrifugal filtration (Waters, 100 kD cutoff) and washing with PBS. The enzymatic activity of the supernatant was monitored by a chromogenic assay (S-2288, Diapharma). After all of the soluble free tPA was removed, the solution was centrifuged (2000 rpm, 10 min) to remove any white precipitate, arising from the degradation of free tPA.

In vitro clot binding

Clots were created from fresh frozen plasma (FFP) in 96 well plates. Each well received 180 μL of FFP, 10 μL of 0.4 M $CaCl_2$, and 10 μL of thrombin (0.1U/μL PBS). The plate was

NIH-PA Author Manuscript

NIH-PA Author Manuscript

NIH-PA Author Manuscript

incubated at 37 °C for 90 min, at which time the respective agent was added. To each clot was then added 6 μg of the nanoparticle preparations (2 mg Fe/mL) which were then incubated at 37 °C for an additional 30 min. The clots were then washed twice with PBS and centrifuged at 500 rpm for 10 minutes. They were then washed twice more with PBS and imaged by fluorescence reflectance imaging in the VT680 channel. All agents containing tPA were pre-incubated with excess PPACK to prevent exogenous tPA-mediated clot lysis.

Amidolytic activity

The amidolytic kinetics of the tested agents were studied with H-D-isoleucyl-L-prolyl-L-arginine-*p*-nitroanilide dihydrochloride (S-2288; Diapharma), a chromogenic substrate as previously described [19]. Free tPA or the nanoagent (both at concentration 0.1×10^{-6} M tPA) was added to the microtiter plate containing assay buffer (0.1 M Tris-HCl, 0.1 M NaCl, pH 8.4) and S-2288 (0.15 – 1.5 mM) at 37 °C. The amidolytic activity was measured at 405 nm for 7 minutes in a microplate reader (Synergy HT, Bio-Tech). The data was plotted as the rate of *p*-nitroanilide release (DA_{405}/min) over substrate concentration and analyzed by analyzed by Michaelis-Menten curve fitting with GraphPad Prism software to access the catalytic efficiency (k_{cat}/K_m, $mM^{-1}s^{-1}$).

In vitro assessment of fibrinolytic activity

In vitro fibrinolytic activity of **CLIO-FXIII-PEG-tPA** was detected by an IMUCLON D-dimer ELISA assay (American Diagnostica Inc., Stamford, CT). Free tPA and **CLIO-FXIII-PEG-tPA** were matched by amidolytic activity in all experiments and were utilized at 4 and 2 ng/mL tPA, as determined by the standard curve. FFP clots were formed as described above and were incubated with the respective agent (10 μL) for 60 min, at which time PPACK (10-fold molar excess) was added to halt further lysis. The clot supernatants were then assayed for D-dimer formation.

Determination of in vivo nanogent binding to arterial and venous thrombi

In vivo thrombi were induced by ferric chloride (topical 7.5% $FeCl_3$) injury to the femoral artery and vein. Mice were anesthetized using an intraperitoneal (IP) ketamine (50 mg/ml, 330 μl), xylazine (100 mg/ml, 50 μl), and sterile saline (380 μl) mixture. Each mouse received a 50 μl IP induction dose of the resulting mixture, followed by 20–30 μl IP hourly for continued anesthesia. After surgical resection of the overlying tissue, $FeCl_3$ was locally applied to the femoral vein using a 1 mm strip of Whatman No.1 filter paper soaked in 7.5% $FeCl_3$ in distilled water as previously reported [10]. The filter paper was applied to the anterior surface of the vein for 5 min. Thereafter, the filter paper was removed and washed with PBS. At 60 min after induction, the respective thrombus-targeted agent (**CLIO-FXIII-PEG-tPA**) or control agent (**CLIO-CXIII-PEG-tPA**) was administered via retro-orbital injection. All agents were injected at 7.5 mg Fe/kg mouse (100 μL total volume). At 90 minutes after thrombus induction, 100 μl of FITC-dextran (5 mg/ml, ex/em 490/525) was co-injected to provide a fluorescence angiogram of the vessels. At 120 minutes after thrombus induction (60 minutes after injection of agent), multichannel intravital fluorescence microscopy (IVFM) was performed.

IVFM studies employed a multichannel laser scanning fluorescence microscope optimized for intravital imaging as previously reported [20]. Excitation beams at wavelengths of 491 nm and 532 nm were generated by a single diode-pumped solid state laser (Dual Calypso, Cobolt AB, Solna, Sweden). The 635 nm excitation light was generated by a diode laser (Radius, Coherent Inc, Santa Clara, CA). These laser beams were deflected into a custom-designed video-rate (30 frames/second) x–y scanner (polygon, galvanometer) and then focused onto the femoral vein with a 17x, N.A.=0.9, water-immersion microscope objective lens (EAF-30-1, LOMO, Northbrook, IL). Each fluorescence signal was epi-collected by a

NIH-PA Author Manuscript

NIH-PA Author Manuscript

NIH-PA Author Manuscript

corresponding photo multiplier tube (R3896, Hamamatsu Photonics, Bridgewater, NJ). The FITC-dextran fluorescence was collected through a 509–547 nm bandpass filter, VT680 fluorescence was collected through a 667–722nm bandpass filter. The two-dimensional images in x–y plane (500×500 pixels) were acquired by a frame grabber (Snapper-8/24 PCI, Active Silicon, North Chelmsford, MA) installed on a Macintosh PC. The imaging speed was 30 frames/sec and each static image was an average of 30 frames. Z-stacks (2.0 μm steps with 700 μm × 700 μm field of view) were collected throughout the entire thrombus region.

Image analysis of IVFM data sets were performed by compiling z-stacks into a 2-dimensional summation image (ImageJ, version 1.36b, Bethesda, MD). Thrombus was identified as filling defects on FITC-dextran generated angiograms. Regions of interest (ROIs) were manually traced within the thrombus and the adjacent normal vessel as previously [21]. The total NIRF signal in the ROI was calculated as the summation of the signal intensity (SI) of all pixels in the ROI. The thrombus target-to-background ratio (TBR) was calculated as the ratio of thrombus SI to the adjacent vessel background SI.

Histology and fluorescence microscopy

After sacrifice, mice were perfused with 0.9% saline (20 ml) via the left ventricle. For histopathological analysis, femoral vessels were embedded in optimal cutting temperature compound (Sakura Finetek, Torrance, CA) and then fresh frozen. Serial 6-μm thick cryostat sections were obtained from embedded femoral veins for fluorescence microscopy. Adjacent sections were stained with hematoxylin and eosin (H&E) for general morphology. Fluorescence microscopy was performed on fresh-frozen femoral vessel sections using an upright epifluorescence microscope (Nikon Eclipse 90i, Tokyo, Japan). Fluorescence images were obtained at a wavelength to detect FITC (filter, 460–500 nm excitation; 510–560 nm emission, exposure time 50.0 ms), or VT680 (filter, 630–670 nm excitation; 685–735 nm emission, exposure time 50.0 ms).

^{125}I-labeling of fibrinogen

Native human fibrinogen (50 mkg; American Diagnostica Inc.) was radioiodinated with [^{125}I]NaI (NEN-Dupont, Boston, MA) in pre-coated Pierce iodination tubes (Thermo Scientific Inc.) by the Iodogen method [22, 23]. ^{125}I-fibrinogen was separated by gel filtration chromatography on a PD-10 column (Pharmacia Biotech. Inc.) with a specific activity of 1.8×10^{6} cpm·mkg^{-1}.

In vitro calibration of thrombolytic activity

Prior to in vivo fibrinolytic evaluation, the **CLIO-FXIII-PEG-tPA** nanoagent was normalized to free tPA by in vitro fibrinolytic activity. To accomplish this, fresh frozen human plasma (45 μl) was mixed with trace amounts of ^{125}I-labeled human fibrinogen (100,000 cpm) and clotted with $CaCl_2$ (20 mM, final concentration) and thrombin (1 IU/ml, final concentration) in 5 ml polystyrene tubes at 37 °C for 60 min. The clots formed were twice washed by 1 ml of PBS (pH 7.4) containing $CaCl_2$ (20 mM) and suspended in 950 μl of human plasma as supernatant. Experiments were started immediately thereafter by adding tPA or nanoagent (50 μl; 0–600 nM). Final concentrations of tPA or nanoagent (0 – 30 nM) were calculated based on their total protein amount and a molecular weight of 68 kDa. The degree of lysis was measured at 1 h, 2 h and 3 h of incubation by γ-counting of supernatant (100 μl) and the fractional fibrinolysis was determined as described [24, 25].

NIH-PA Author Manuscript

NIH-PA Author Manuscript

NIH-PA Author Manuscript

Assessment of in vivo thrombolysis in murine pulmonary embolism

Thrombolytic studies were performed as described previously in a humanized mouse model [23]. Human plasma (25 μl) was mixed with trace amounts of ^{125}I-labeled human fibrinogen (300,000 cpm) and clotted in PE50 tubing (Clay Adams, PE-50, Becton Dickinson, Sparks, MD) with $CaCl_2$ (20 mM) and thrombin (0.1 units) at 37 °C for 60 min. The clots were measured by a γ-scintillation counter prior to embolization in order to determine the initial radioactivity. Wild type female mice (C57BL/6J, 10–14 wks) were anesthetized by pentobarbital (IP, 70 mg/kg). The right and left internal jugular veins were exposed. The left vein was used to embolize the thrombus and to supplement the mouse with human plasminogen (14 mg/kg); the right vein was used for infusion of heparin (100 U/kg) and free tPA (n = 9) or **CLIO-FXIII-PEG-tPA** (n = 11). Prior to injection, fibrinolytic agents were normalized by in vitro fibrinolytic activity as above. Control animals (n = 6) were similarly treated only with heparin (100 U/kg) in sterile saline solution. Two hours after embolization mice were sacrificed by CO_2 inhalation. The heart and lungs were dissected and γ-counted to determine the amount of residual thrombus radioactivity. The amount of lysis was measured and computed using the following equation: percent lysis = 100% × (embolized clot cpm − residual clot cpm)/(embolized clot cpm).

Results and discussion

Synthesis and characterization of the nanoagents

The thrombolytic nanoagent and respective controls were synthesized in a layer-by-layer manner, as depicted in Scheme 1. CLIO was initially modified with the succinimidyl ester of VivoTag 680 (VT680), to impart upon the particle the ability to be fluorescently monitored. Subsequently, the agent was reacted with succinimidyl iodoacetate to allow for conjugation of the targeting peptide to the particle surface via a thioether linkage. The activated factor XIII-targeted peptide (FXIII), GNQEQVSPLTLLKC-NH_2, was derived from the N-terminus of α_2-antiplasmin, and has been shown to be actively crosslinked into acute clots by the transglutaminase via the glutamine-14 residue. The control peptide, GNAEQVSPLTLLKC-NH_2, contains a single amino acid mutation of the glutamine-14 residue to alanine, which ablates it binding capacity [12, 13]. It should be noted that the N-terminus of the peptide sequences are unprotected, which allows for subsequent modification. As opposed to thrombus-targeted agents where the targeting moiety is non-covalently bound, the FXIII peptide covalently modifies the clot. This also allows for continual accumulation of the agent without any appreciable dissociation, unless clot lysis occurs. The number of peptides per particle was ascertained by the labeling of the N-terminus of a small portion of the product with fluorescein isothiocyanate and spectroscopic quantification, resulting in 34 peptides per particle, and a minimum increase in hydrodynamic diameter (51.3 nm for CLIO-VT680 versus 59.0 nm for the peptide-modified derivative).

Next, a discrete polyethylene glycol (PEG) spacer moiety was added to increase the distance between the fibrinolytic drug and the particle to minimize steric interactions. Whereas the main goal in the modification of the nanoagent with a targeting peptide was the maximum loading of the particle surface that yields a stable conjugate, the addition of the PEG linker moiety must occur in a substoichiometric ratio (per peptide). This ensures that the avidity of the nanoparticle for thrombi is not significantly affected by the inclusion of the therapeutic moiety. Reaction of the succinimidyl ester of a maleimide-modified PEG with the peptide modified nanoparticle result in approximately 21 PEG per particle, as determined spectroscopically after labeling the maleimide moiety of a small amount of the product with a thiol-modified fluorescein derivative. This nanoparticle was then reacted with tPA. Interestingly, tPA contains one free cysteine in the growth factor domain (Cys 83), which

NIH-PA Author Manuscript

NIH-PA Author Manuscript

NIH-PA Author Manuscript

allows for modification via thioether formation. Thus, the enzyme is only modified in one manner, which ensures homogeneity. Purification of the final products was facilitated by centrifugal filtration with a 100 kDa cutoff membrane, providing for the removal of the free tPA from that bound to the nanoparticle. An additional non-targeted control nanoagent (**CLIO-PEG-tPA**) was also synthesized via the same methodology without the inclusion of the targeting peptide. Overall, the particle diameter increased modestly to 63.9 nm, as could be expected for the appending of a protein 5 nm in diameter to the particle surface.

The clot-binding ability of the nanoagents was investigated at each stage of synthesis toensure that the modifications did not have deleterious effects on the particle targeting efficiency. Clots were formed in vitro by addition of thrombin and $CaCl_2$ to fresh frozen plasma (FFP). The agents were then incubated with the clots, washed vigorously, and imaged by fluorescence reflectance imaging (FRI). Importantly, the tPA moiety of each agent was neutralized by preincubation with PPACK, a tri-peptide chloromethylketone based tPA inhibitor, to prevent dissolution of the clots during the experiment. As can be seen in figure 1, all agents displayed at least some baseline fluorescence signal, as compared to clots incubated with phosphate buffered saline (PBS), yet the FXIII-targeted agents possessed significantly higher target-to-background (TBR) ratios at each stage of the synthesis (TBR of 9.8 for CLIO-FXIII-PEG-tPA versus 4.5 for CLIO-PEG-tPA and 3.7 for CLIO-CXIII-PEG-tPA, ANOVA $p < 0.05$). The background fluorescence of the non-targeted agents can be likely attributed to non-specific adherence of the CLIO-based agents to the plasma clots.

The number of tPA molecules per particle was next characterized using the Bradford protein assay. The concentration of the protein was determined using both bovine serum albumin and free tPA as standards, and demonstrated the conjugation of 3–4 molecules of tPA to each peptide-modified particle (**CLIO-FXIII-PEG-tPA** and **CLIO-CXIII-PEG-tPA**). Interestingly, the non-peptide modified conjugate, **CLIO-PEG-tPA**, bore slightly less than 1 tPA per particle. This may be attributed to the different particle surfaces that are present during the addition of the PEG moiety (i.e. a relatively hydrophobic peptide versus a polycationic hydrophilic polymer), as the reaction conditions were otherwise identical. Due to these substantial differences in tPA loading, **CLIO-PEG-tPA** was not investigated further in this study. The enzymatic efficiencies of the remaining peptide-modified conjugates were examined. Serine protease activity was initially tested using S-2288, a chromogenic assay for tPA amidolytic efficiency. As compared to free tPA, the CLIO-based tPA conjugates demonstrated a 15% decrease in overall efficiency on a weight basis (Figure 2A). This finding may be due to steric constraints introduced by the conjugation strategy or the presence of the considerably larger CLIO nanoparticle. The fibrinolytic capacity of the targeted (**CLIO-FXIII-PEG-tPA**) agent were subsequently tested in vitro with a D-dimer assay. D-dimer is a soluble fibrin degradation product that is formed during fibrinolysis. Clinically, the D-dimer level can be utilized as a screening blood test to determine whether or not a thrombus is present in a patient, and when low, the D-dimer test has a high negative predictive value. In this experiment FFP clots were incubated with the respective agents for 60 min, at which time the supernatant was removed and assayed for the presence of D-dimer. When the amidolytic activities of the conjugates were matched, as determined by the S2288 chromogenic assay, the nanoagent generated D-dimer levels comparable to free tPA (Figure 2B), indicating similar in vitro thrombolytic efficacy. Notably, this experiment was performed under static (non-flowing) conditions, thus the potentially advantageous targeting ability of **CLIO-FXIII-PEG-tPA** was not realized.

NIH-PA Author Manuscript

NIH-PA Author Manuscript

NIH-PA Author Manuscript

In vivo thrombus binding

The in vivo targeting ability of the nanoagents was tested in a murine model of arterial and venous thrombosis, in which the femoral artery and vein were exposed via surgical dissection and a strip of filter paper soaked in $FeCl_3$ was applied to the vessel surface. This resulted in endothelial damage and local thrombus formation. One hour after the induction of thrombosis, the mice were injected with either the targeted or the control agent, which was allowed to circulate for one hour prior to intravital fluorescence microscopy (IVFM). Immediately prior to imaging, the mice were also injected with a high molecular weight fluorescein-labeled dextran (FITC-dextran) to delineate the vasculature and thrombus location. *Whereas the active agents were injected in all experiments, thrombolysis was not expected as murine plasminogen system is 10-fold less sensitive to human tPA* [26, 27]. *Thus, this experiment focused solely upon nanoagent localization.*

As is shown in Figure 3, **CLIO-FXIII-PEG-tPA** readily targeted intravascular thrombi (Figure 3A), as compared to the control agent, **CLIO-CXIII-PEG-tPA** (Figure 3B). While FITC-dextran delineated the vasculature (green), **CLIO-FXIII-PEG-tPA** appeared as a fluorescent signal (red) along the periphery of the clot. As seen in previous experiments with the thrombus-targeted, nonfibrinolytic magnetofluorescent nanoagents [10], these agents did not penetrate the full thickness of the clot, and were instead restricted to the luminal surface of the thrombus. Figure 3G schematically illustrates the resulting effect, where the center of the thrombus will appear dark, yet which results in a ring of fluorescence intensity around the thrombus, corresponding to nanoagent binding. This surface binding effect is not restricted to larger nanoparticulate vehicles, as this has also been observed with low molecular weight peptide-based imaging agents [12]. Whereas clots are somewhat porous, the rate of blood flow through them is negligible, as compared to the luminal surface of a non-occlusive thrombus. Therefore delivery of any molecule to the center of a clot will be a diffusion-limited process, thereby favoring surface binding. This is similar to what is observed in thrombolysis, as clots are also known to be lysed from the outside-in [28–30].

The TBRs of the nanoagents were examined in both arterial and venous thrombi. For venous thrombosis, **CLIO-FXIII-PEG-tPA** demonstrated 2.5 fold greater TBR versus the control agent (2.3 ± 0.80 vs 0.83 ± 0.27, $p < 0.001$ Figure 3E), while in arterial thrombi it showed a 2 fold greater TBR (1.6 ± 0.26 vs 0.8 ± 0.22, $p < 0.001$, Figure 3F). This binding was further confirmed histologically. As can be seen in figure 3C, fluorescence signal in the VT680 channel colocalized with the shoulder regions of the thrombus, while negligible thrombus binding was observed in mice that received **CLIO-CXIII-PEG-tPA**.

In vivo thrombolysis of pulmonary emboli

The in vivo fibrinolytic capacity of **CLIO-FXIII-PEG-tPA** was then studied in a "humanized" murine pulmonary embolism model [23]. *As opposed to the previous study, where four fibrinolytic agents with different mechanisms of action were used, tPA is the sole PA employed in this study. Thus, wild type mice were used in all experiments, as plasminogen deficient mice were not required to negate the differing activation mechanisms.* The pulmonary embolization was achieved by injection of a preformed ^{125}I-labeled human plasmaclot to the mouse jugular vein. The clot lysis was assessed by the supplementation of murine fibrinolytic system with human plasminogen and administration of either free tPA or the thrombolytic nanoagent **CLIO-FXIII-PEG-tPA**. *Compared to $FeCl_3$-induced femoral thrombosis, embolization of ^{125}I-fibrin clot may produce clot deposition in either the pulmonary artery, the right ventricle, or both. This variability complicates a functional measurement of the restoration of blood flow. Thus, this experimental protocol was designed to estimate the clot lysis capacity of a fibrinolytic agent in vivo.* Two hours after embolization, the mice were sacrificed, and the heart and lungs were removed and analyzed

NIH-PA Author Manuscript

NIH-PA Author Manuscript

NIH-PA Author Manuscript

for residual thrombus radioactivity. As can be seen in Figure 4A, the injection of equivalent amounts of tPA (on a mass basis) demonstrated that the efficacy of the targeted nanoagent was preserved, albeit at slightly lower levels when compared to free tPA. This is likely due to steric hindrance, and was consistent also with the observed decrease in amidolytic efficiency demonstrated above (Figure 2). Yet, the injected dose of any enzyme-based therapeutic is routinely normalized by its net activity, rather than mass [31]. Thus, when the obtained data is calibrated based on intrinsic fibrinolytic activity, via the in vitro dissolution of ^{125}I-labeled clots, the **CLIO-FXIII-PEG-tPA** agent proved as efficient at lysing clots as free tPA (Figure 4B).

Traditionally, the targeting of a therapeutic moiety to the site of action aims to increase local therapeutic activity. In this case, parity between the free thrombolytic and the targeted nanothrombolytic is likely the result of the PA (tPA) used. tPA was employed as it is widely utilized worldwide for diverse fibrinolytic indications. However unlike nonspecific PAs such as streptokinase, tPA is a fibrin-specific thrombolytic that requires binding to fibrin prior to the conversion of plasminogen to plasmin, and subsequent fibrinolysis. Although its constitution allowed for a facile conjugation strategy, the steric bulk associated with its conjugation to a nanoparticulate scaffold could potentially decrease its binding to fibrin, thereby decreasing its overall activity, an effect that was not evident at the projects' conception. A nanolytic approach utilizing other fibrin non-specific PAs such as streptokinase may enable superior fibrinolytic efficacy.

Conclusions

We have demonstrated the development a FXIIIa thrombus-targeted nanoagent (**CLIO-FXIII-PEG-tPA**) for the efficient delivery of a PA to the desired site of action. This thrombolytic nanoagent was shown to efficiently bind to clots in vitro, with a minimal decrease in overall amidolytic and fibrinolytic activity, as compared to free tPA. Intravital fluorescence microscopy leveraged the theranostic capabilities of the nanoagent and demonstrated binding to the thrombus edge in both arterial and venous thrombosis. When utilized in vivo in a murine model of pulmonary embolism, the targeted nanoagent readily lysed clots, demonstrating efficacy comparable to free tPA. While this report does not demonstrate superiority of the nanoagent versus the parent thrombolytic, it is a promising proof-of-principle example of thrombus-targeted fibrinolytic agent with theranostic capabilities, as demonstrated here for optical imaging, and previously for magnetic resonance imaging [10]. Potential advantages of the synthesized agent may be in its overall safety profile. One of the main complications that arises in the use of PAs is the impairment of hemostasis which may lead to life-threatening bleeding, especially intracerebral hemorrhage. Nanoagents, for the most part, have difficulty in passing through the blood brain barrier (BBB), as exemplified by the significant amount of research that has gone into developing BBB-transversing nanomaterials [8]. Thus, the marriage of a thrombolytic to nanomaterials may lead to PAs with diminished detrimental side effects. Examination of these relevant off-target effects of these nanoagents in experimental hemorrhage models is currently planned.

Future perspective

With regard to thrombolytic therapies, significant advancements have been made in order to increase the efficacy of plasminogen activators. The evolution from fibrin non-specific to fibrin-specific therapeutics was the first step, allowing for a decrease in the activation of circulating plasminogen. This has been followed by the reengineering of the PA in order to modulate its blood half life. Recombinant tPA, which was utilized in this study, is often given as an infusion over the course of 90 min, as its blood half life is 4–6 min [9].

NIH-PA Author Manuscript

NIH-PA Author Manuscript

NIH-PA Author Manuscript

Tenecteplase, which was approved by the FDA as a fibrinolytic agent in 2000, is given as a single bolus, may take 20–24 min to clear from the blood, has higher fibrin specificity, yet still demonstrates similar ICH rates as tPA of ~1% in acute myocardial infarction patients [9]. Thus, the design of nanoagents with comparable therapeutic efficacy to the free drugs, yet demonstrating superior safety profiles may provide for the easing of the complications often associated with PA therapies, particularly intracerebral hemorrhage, as nanoagents with minimal blood brain barrier permeability can be utilized to develop targeted thrombolytics.

Ethical conduct of research

The authors state that they have obtained appropriate institutional review board approval or have followed the principles outlined in the Declaration of Helsinki for all human or animal experimental investigations. In addition, for investigations involving human subjects, informed consent has been obtained from the participants involved.

Acknowledgments

This work was supported in part with funds from the NIH NHLBI under grant number R21HL093607 (JM), R01 HL108229 (FJ), U01-HL080731 (JM, FJ, GR, RW) and contract number HHSN268201000044C (JM, RW), the American Heart Association Scientist Development Grant 0830309N (IS) the American Heart Association Scientist Development Grant 0830352N (FJ), and the Howard Hughes Medical Institute Career Development Award (FJ).

References

1. Anderson HV, Willerson JT. Thrombolysis in acute myocardial infarction. N Engl J Med. 1993; 329:703–709. [PubMed: 8345856]
2. Tissue plasminogen activator for acute ischemic stroke. The National Institute of Neurological Disorders and Stroke rt-PA Stroke Study Group. N Engl J Med. 1995; 333:1581–1587. [PubMed: 7477192]
3. Armstrong PW, Collen D. Fibrinolysis for acute myocardial infarction: current status and new horizons for pharmacological reperfusion, part 1. Circulation. 2001; 103:2862–2866. [PubMed: 11401946]
4. Marsh JN, Hu G, Scott MJ, et al. A fibrin-specific thrombolytic nanomedicine approach to acute ischemic stroke. Nanomedicine (Lond). 2011; 6:605–615. [PubMed: 21506686]
5. Bi F, Zhang J, Su Y, Tang YC, Liu JN. Chemical conjugation of urokinase to magnetic nanoparticles for targeted thrombolysis. Biomaterials. 2009; 30:5125–5130. [PubMed: 19560812]
6. Ma YH, Wu SY, Wu T, Chang YJ, Hua MY, Chen JP. Magnetically targeted thrombolysis with recombinant tissue plasminogen activator bound to polyacrylic acid-coated nanoparticles. Biomaterials. 2009; 30:3343–3351. [PubMed: 19299010]
7. Marsh JN, Senpan A, Hu G, et al. Fibrin-targeted perfluorocarbon nanoparticles for targeted thrombolysis. Nanomed. 2007; 2:533–543.
8. Silva GA. Nanotechnology approaches to crossing the blood-brain barrier and drug delivery to the CNS. BMC Neurosci. 2008; 9 (Suppl 3):S4. [PubMed: 19091001]
9. Ross AM. New plasminogen activators: a clinical review. Clin Cardiol. 1999; 22:165–171. [PubMed: 10084057]
10. McCarthy JR, Patel P, Botnaru I, Haghayeghi P, Weissleder R, Jaffer FA. Multimodal nanoagents for the detection of intravascular thrombi. Bioconjug Chem. 2009; 20:1251–1255. [PubMed: 19456115]
11. Robinson BR, Houng AK, Reed GL. Catalytic life of activated factor XIII in thrombi Implications for fibrinolytic resistance and thrombus aging. Circulation. 2000; 102:1151–1157. [PubMed: 10973845]
12. Jaffer FA, Tung CH, Wykrzykowska JJ, et al. Molecular imaging of factor XIIIa activity in thrombosis using a novel, near-infrared fluorescent contrast agent that covalently links to thrombi. Circulation. 2004; 110:170–176. [PubMed: 15210587]

NIH-PA Author Manuscript

NIH-PA Author Manuscript

NIH-PA Author Manuscript

13. Tung CH, Ho NH, Zeng Q, et al. Novel factor XIII probes for blood coagulation imaging. ChemBioChem. 2003; 4:897–899. [PubMed: 12964167]
14. Miserus RJ, Herias MV, Prinzen L, et al. Molecular MRI of early thrombus formation using a bimodal alpha2-antiplasmin-based contrast agent. JACC Cardiovasc Imaging. 2009; 2:987–996. [PubMed: 19679287]
15. Josephson L, Tung CH, Moore A, Weissleder R. High-efficiency intracellular magnetic labeling with novel superparamagnetic-Tat peptide conjugates. Bioconjug Chem. 1999; 10:186–191. [PubMed: 10077466]
16. Palmacci, S.; Josephson, L. Synthesis of polysaccharide covered superparamagnetic oxide colloids. 5,262,176. 1993.
17. Perez JM, O'Loughin T, Simeone FJ, Weissleder R, Josephson L. DNA-based magnetic nanoparticle assembly acts as a magnetic relaxation nanoswitch allowing screening of DNA-cleaving agents. J Am Chem Soc. 2002; 124:2856–2857. [PubMed: 11902860]
18. Zuckermann R, Corey D, Schultz P. Efficient methods for attachment of thiol specific probes to the 3′-ends of synthetic oligodeoxyribonucleotides. Nucleic Acids Res. 1987; 15:5305–5321. [PubMed: 3601673]
19. Machado LS, Sazonova IY, Kozak A, et al. Minocycline and tissue-type plasminogen activator for stroke: assessment of interaction potential. Stroke. 2009; 40:3028–3033. [PubMed: 19628804]
20. Veilleux I, Spencer JA, Biss DP, Cote D, Lin CP. Cell tracking with video rate multimodality laser scanning microscopy. IEEE Journal of Selected Topics in Quantum Electronics. 2008; 14:10–18.
21. Chang K, Francis SA, Aikawa E, et al. Pioglitazone suppresses inflammation in vivo in murine carotid atherosclerosis: novel detection by dual-target fluorescence molecular imaging. Arterioscler Thromb Vasc Biol. 2010; 30:1933–1939. [PubMed: 20689078]
22. Fraker PJ, Speck JCJ. Protein and cell membrane iodinations with a sparingly soluble chloroamide, 1,3,4,6-tetrachloro-3a,6a-diphrenylglycoluril. Biochem Biophys Res Commun. 1978; 80:849–857. [PubMed: 637870]
23. Sazonova IY, McNamee RA, Houng AK, King SM, Hedstrom L, Reed GL. Reprogrammed streptokinases develop fibrin-targeting and dissolve blood clots with more potency than tissue plasminogen activator. J Thromb Haemost. 2009; 7:1321–1328. [PubMed: 19566545]
24. Colucci M, Scopece S, Gelato AV, Dimonte D, Semeraro N. In vitro clot lysis as a potential indicator of thrombus resistance to fibrinolysis--study in healthy subjects and correlation with blood fibrinolytic parameters. Thromb Haemost. 1997; 77:725–729. [PubMed: 9134650]
25. Turner RB, Liu L, Sazonova IY, Reed GL. Structural elements that govern the substrate specificity of the clot-dissolving enzyme plasmin. J Biol Chem. 2002; 277:33068–33074. [PubMed: 12080056]
26. Korninger C, Collen D. Studies on the specific fibrinolytic effect of human extrinsic (tissue-type) plasminogen activator in human blood and in various animal species in vitro. Thromb Haemost. 1981; 46:561–565. [PubMed: 6795744]
27. Lijnen HR, van Hoef B, Beelen V, Collen D. Characterization of the murine plasma fibrinolytic system. Eur J Biochem. 1994; 224:863–871. [PubMed: 7523120]
28. Diamond SL, Anand S. Inner clot diffusion and permeation during fibrinolysis. Biophys J. 1993; 65:2622–2643. [PubMed: 8312497]
29. Francis CW, Marder VJ. A molecular model of plasmic degradation of crosslinked fibrin. Semin Thromb Hemost. 1982; 8:25–35. [PubMed: 6460319]
30. Veklich Y, Francis CW, White J, Weisel JW. Structural studies of fibrinolysis by electron microscopy. Blood. 1998; 92:4721–4729. [PubMed: 9845538]
31. Runge MS, Bode C, Matsueda GR, Haber E. Antibody-enhanced thrombolysis: targeting of tissue plasminogen activator in vivo. Proc Natl Acad Sci U S A. 1987; 84:7659–7662. [PubMed: 3118374]

NIH-PA Author Manuscript

NIH-PA Author Manuscript

NIH-PA Author Manuscript

Executive summary

- Targeted nanoparticulate delivery vehicles can be utilized to deliver thrombolytics to sites of action.
- Covalent functionalization of CLIO targeted to clots via a FXIII specific peptide with tPA results in a nanoagent (**CLIO-FXIII-PEG-tPA**) that retains avid clot binding, yet demonstrates a mild decrease in S2288-determined amidolytic efficiency, plausibly due to steric constraints.
- S2288 amidolytic efficiency-matched samples of the targeted thrombolytic nanoagent and free tPA demonstrate comparable clot lysis in vitro.
- In vivo, the peptide-targeted thrombolytic nanoagent backbone readily binds arterial and venous thrombi, as determined by IVFM detection of the theranostic agent.
- In a murine model of pulmonary embolism, the targeted nanoagent displays thrombolytic potential comparable to free tPA, when matched for in vitro fibrinolytic activity
- This class of targeted thrombolytic nanoagents may ultimately prove more efficacious due to improved safety profiles.

NIH-PA Author Manuscript

NIH-PA Author Manuscript

NIH-PA Author Manuscript

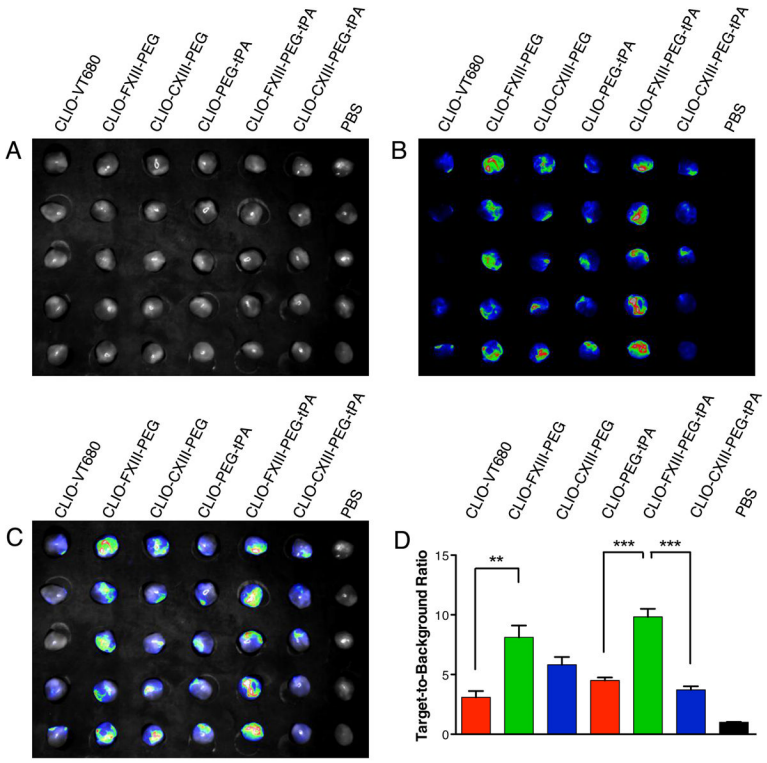

Figure 1.

In vitro binding of synthesized nanoagent to FFP clots. A) White light image of FFP clots; B) Fluorescence reflectance image of nanoagent binding in the VT680 channel; C) Merged white light and fluorescence images depicting clot binding; D) Quantification of clot target-to-background ratio. All results relative to PBS-treated clots. (** P = 0.0017, *** P < 0.0001)

NIH-PA Author Manuscript

NIH-PA Author Manuscript

NIH-PA Author Manuscript

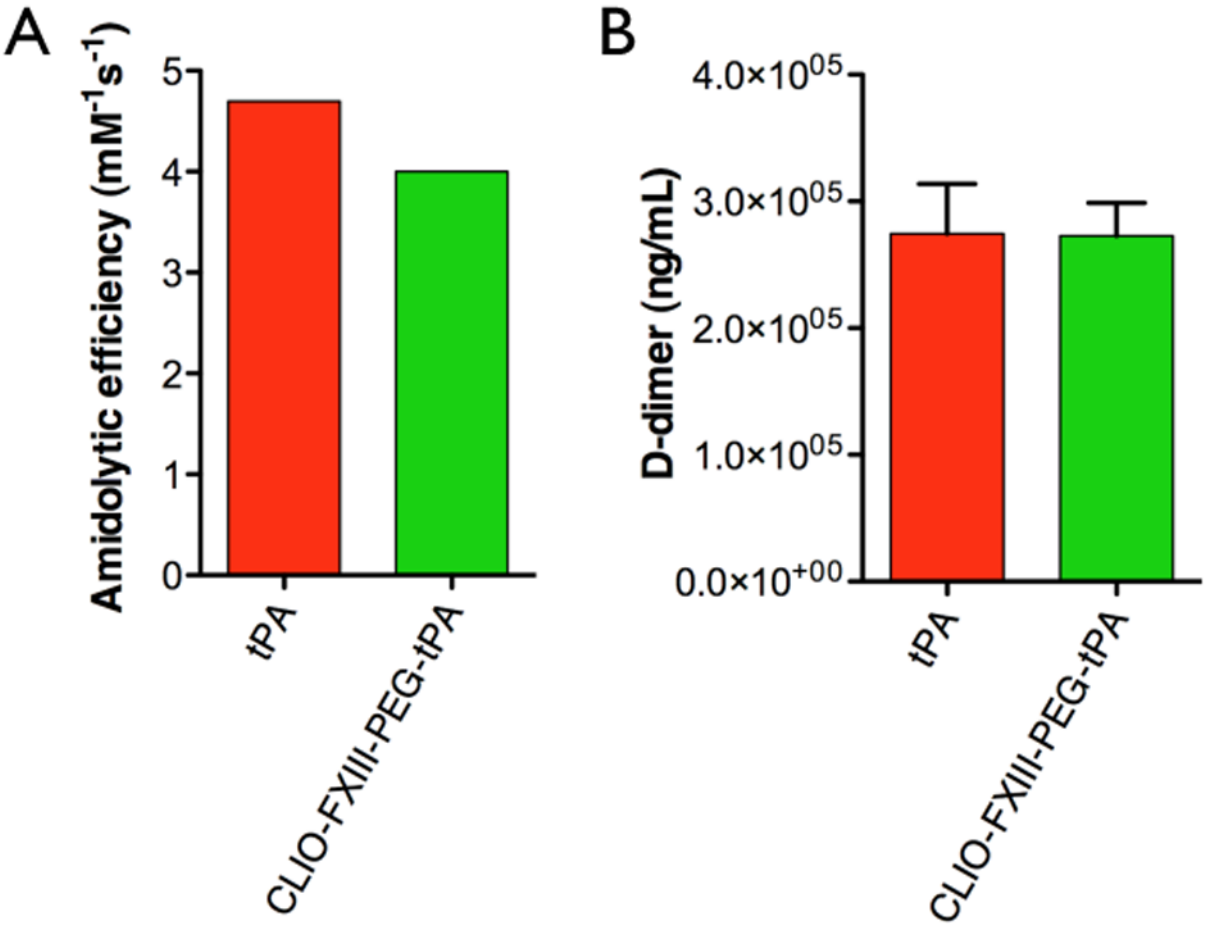

Figure 2.

Amidolytic and fibrinolytic potential of the synthesized nanoagents. A) Amidolytic efficiency decreased by 15% upon conjugation of tPA to the CLIO nanoscaffold, as determined by the S-2288 chromogenic assay. B) When fibrinolysis of activity matched samples of **CLIO-FXIII-PEG-tPA** and free tPA were assayed by D-dimer ELISA, the nanoagent demonstrated equivalent lytic efficacy ($p > 0.05$).

NIH-PA Author Manuscript

NIH-PA Author Manuscript

NIH-PA Author Manuscript

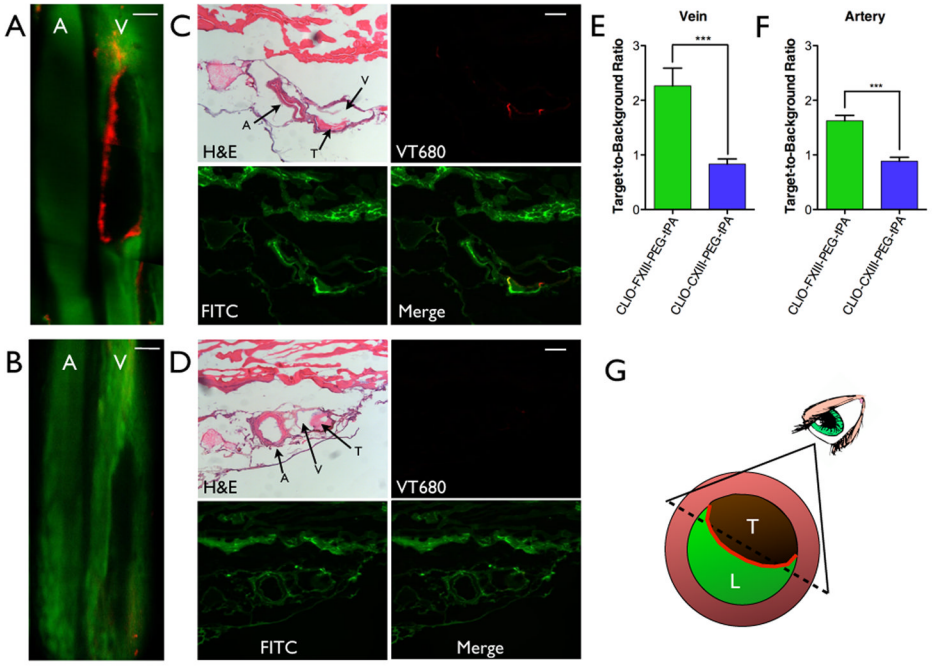

Figure 3.

In vivo examination of nanoagent binding to arterial and venous thrombi. Representative IVFM images of the localization to intravascular thrombi of **CLIO-FXIII-PEG-tPA** (A) and **CLIO-CXIII-PEG-tPA** (B) demonstrating significant binding of the FXIIIa-targeted agent to the periphery of the thrombus (Scale bar = 100 μm). Histological examination of **CLIO-FXIII-PEG-tPA** (C) and **CLIO-CXIII-PEG-tPA** (D) localization (Scale bar = 100 μm). In A–D, green fluorescence can be attributed to fluorescein-labeled dextran, which is used to delineate the vasculature, while red fluorescence is attributable to the fluorophore on the nanoparticle. Target-to-background ratios were calculated for the veins (E) and arteries (F) in all in vivo experiments. G) Schematic diagram representing IVFM imaging results. While the lumen contains FITC-dextran as a means to assess the vasculature (green), the targeted nanoagent binds to the luminal surface of the thrombus (red). The IVFM field of view results in an edge effect for **CLIO-FXIII-PEG-tPA** binding with no fluorescence from the center of the thrombus. Scale bars, 100 μm. (*** $P < 0.0001$) *A = artery, V = vein, T = thrombus, L = lumen.*

NIH-PA Author Manuscript

NIH-PA Author Manuscript

NIH-PA Author Manuscript

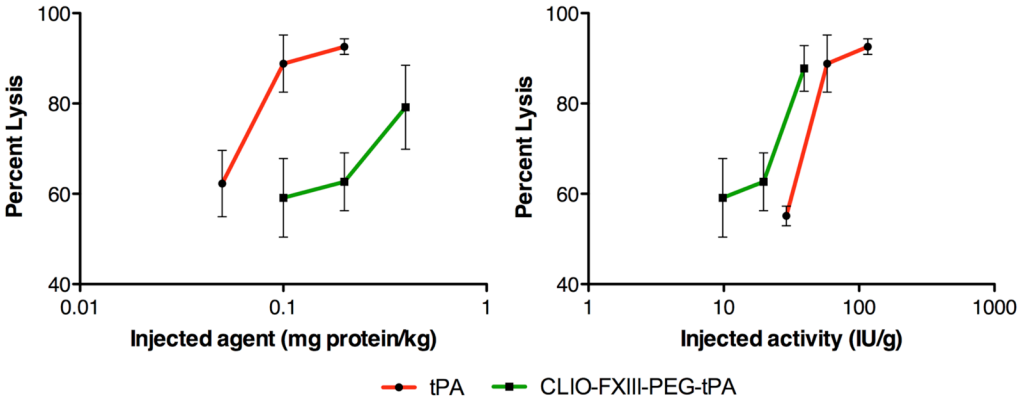

Figure 4.

In vivo fibrinolysis of murine pulmonary emboli. Whereas thrombolytic efficacy of **CLIO-FXIII-PEG-tPA** is less than free tPA on a weight basis (A), after the thrombolytic activity is normalized by in vitro clot lysis capacity (B) the **CLIO-FXIII-PEG-tPA** agent is equally as efficient as free tPA at lysing clots.

NIH-PA Author Manuscript

NIH-PA Author Manuscript

NIH-PA Author Manuscript

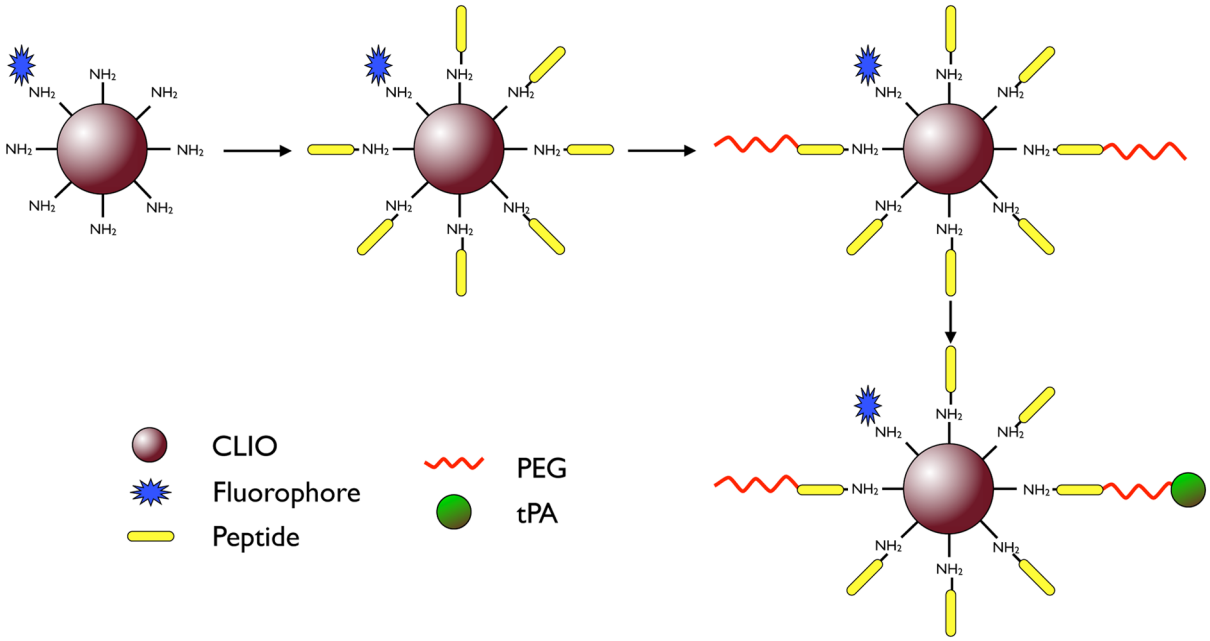

Scheme 1.
Layer-by-layer synthesis of thrombolytic nanoagents.